

Observation of Selenium-77 Nuclear Magnetic Resonance in Octaneselenol-Protected Gold Nanoparticles

Brian S. Zelakiewicz,[†] Tetsu Yonezawa,[‡] and YuYe Tong^{*,†}*Department of Chemistry, Georgetown University, 37th and "O" Streets NW, Washington, DC 20057, and**Department of Chemistry, School of Science, The University of Tokyo, Bunkyo, Tokyo 113-0033, Japan*

Received January 26, 2004; E-mail: yyt@georgetown.edu

Alkaneselenols, or dialkyl-diselenides, offer an interesting alternative chemical motif to, if not better than, the widely used alkanethiols for the formation of self-assembled monolayers (SAMs) on metal surfaces.^{1–3} They can also be used as the protecting ligands to form monolayer-protected metal nanoparticles.^{4,5} In addition, selenium appears to be a better candidate^{6,7} than sulfur for the so-called molecular "alligator clip" (MAC)⁸ in anchoring an organic molecular wire to a metal surface in the context of molecular electronics.⁹ Surprisingly, however, albeit their appealing fundamental as well as practical importance, they have thus far been subject to much less intensive investigations than thiols. Consequently, little is known about the chemistry of alkaneselenol SAM, in particular the metal–selenium MAC bonding interaction. As the first step toward the long-term goal of achieving a better molecular level understanding of the chemistry of metal–MAC bonding interactions, we report here the first observation of ⁷⁷Se nuclear magnetic resonance (NMR) in octaneselenol-protected gold (Au) nanoparticles. The ⁷⁷Se NMR characteristics observed, i.e., broad line shape, unusual fast nuclear spin–lattice and spin–spin relaxation rates, reminiscent of ¹³C NMR of CO chemisorbed on transition metal surfaces (vide infra),¹⁰ strongly suggest the existence of conducting electrons at the Se atom, spilled over from the metal nanoparticles.

Our octaneselenol-protected Au nanoparticles were synthesized using the well-established two-phase procedure pioneered by Schriffin and co-workers,¹¹ but with dioctyl-diselenide as the starting reactant. The purity of the final Au nanoparticles was checked by ¹H and ¹³C NMR in order to make sure that the remaining surfactant and dioctyl-diselenide, if any, are below the detectable limits. The dioctyl-diselenide used in the Au nanoparticle synthesis was made by a two-step process in which selenobenzamide was first synthesized and dioctyl-diselenide was then produced via a reaction between selenobenzamide and 1-bromooctane in anhydrous ethanol under nitrogen.^{12,13} The purity of the product was verified by ¹H and ⁷⁷Se NMR. The Au nanoparticles so synthesized show dominantly a spherical morphology, as demonstrated by the transmission electronic microscopy (TEM) measurements, Figure 1A. In Figure 1B, we show the corresponding particle size distribution which gives an average diameter of 2.5 nm. The corresponding UV–vis spectrum is presented in Figure 1C. The clear appearance of a surface plasma resonance at about 510 nm indicates that the metal core is in a metallic state. Also, the very similar infrared and proton-decoupled ¹³C (natural abundance) NMR spectra of the octaneselenol-protected Au nanoparticles compared to those of octanethiol-protected ones indicate that the aliphatic chains in the former are in an extended, all-trans configuration.¹⁴

All ⁷⁷Se NMR (76.2905 MHz) measurements reported in this communication were carried out at room temperature (298 K) on

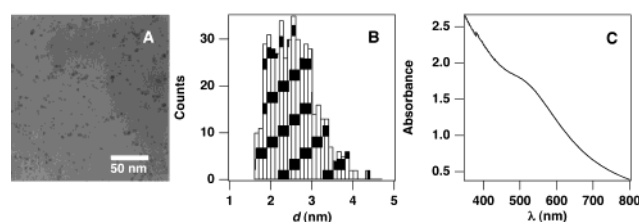


Figure 1. TEM image (A), the corresponding size distribution (B), and the UV–vis spectrum (C) of the octaneselenol-protected Au nanoparticles.

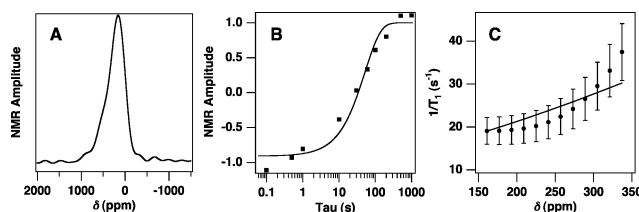


Figure 2. (A) ⁷⁷Se NMR spectrum of octaneselenol-protected Au nanoparticles. (B) Inversion–recovery ⁷⁷Se spin–lattice relaxation curve measured at the peak position, 169 ppm. (C) Typical spin–lattice relaxation rates as a function of the NMR shift. The solid curve is the fit to eq 1.

a "home-assembled" spectrometer equipped with an active-shielded 9.395-T widebore superconducting magnet (Oxford Instruments, Osney Mead, Oxford, UK), Tecmag (Houston, TX) Libra data acquisition system, and a home-built single-channel solenoid probe. The NMR sample consisted of the concentrated C₆D₆ solution of octaneselenol-protected Au nanoparticles contained in an NMR sample vial, 7 mm in diameter and 20 mm in length. To increase the signal over noise ratio, eight echoes were added together per acquisition scan using a CPMG pulse sequence with an eight-phase cycling. The interval between the $\pi/2$ (6 μ s) and π pulses was 50 μ s, the repetition time was 0.25 s, and a typical number of scans was 40 000. Phenylselenol (152 ppm) was used as the secondary reference. The first room-temperature ⁷⁷Se NMR spectrum of octaneselenol-protected Au nanoparticles is shown in Figure 2A. The wiggle of the baseline is caused by the truncation of the time-domain data points required for the echo addition. The spectrum peaks at 169 ppm, with a line width of about 450 ppm. Similarly sized line width was obtained if a normal Hahn-echo sequence without time-domain data-point truncation was used. Such a broad line width is in great contrast to that of ¹³C₁ in the octanethiol-protected Au nanoparticles whose value is about 30 ppm.¹⁵ However, a similarly significant line-broadening has been ubiquitously observed for the ¹³C NMR spectrum of CO adsorbed onto transition metal surfaces with a C-down bonding configuration.¹⁰ Thus, a line-broadening of 450 ppm is consistent with a Se-down bonding scheme and reflects the surface heterogeneity due to the variations in local chemical environment and orientational dependence of magnetic susceptibility of metal nanoparticles as seen by ⁷⁷Se.

[†] Georgetown University.[‡] The University of Tokyo.

Figure 2B shows the ^{77}Se nuclear spin–lattice relaxation curve measured at the peak position and room temperature (298 K) using an inversion–recovery method. The solid curve is the single-exponential fit that gives a relaxation rate of $19 \pm 3 \text{ s}^{-1}$. This is about 5 times faster than the spin–lattice relaxation rate of $^{13}\text{C}_1$ in the octanethiol-protected Au nanoparticles of a similar particle size.¹⁵ The spin–spin relaxation rate at 169 ppm is $3030 \pm 200 \text{ s}^{-1}$, which is about 6–10 times faster than that for $^{13}\text{C}_1$.¹⁵ Since no protons are attached to the Se, C_1 is not enriched, and the natural abundance of ^{77}Se is only 7.6%, then the nuclear dipolar relaxation channel caused by particle tumbling is expected to be much less efficient than that for the $^{13}\text{C}_1$. The fact that this is not the case observed here points toward the other relaxation mechanisms. The most plausible one is the conduction electrons that come from the metal side; i.e., the Fermi level local density of states (E_F -LDOS) at the Se becomes nonzero when bound to Au nanoparticle surfaces.

It has been well established previously that the ^{13}C NMR characteristics of the CO chemisorbed onto transition metal nanoparticle surfaces are mainly determined by the magnetic interactions between the ^{13}C nuclear spin and that of the conducting electron.¹⁰ This is because the surface chemical bonding generates nonzero E_F -LDOS at the C atom; therefore, both the ^{13}C spin–lattice and spin–spin relaxations become distinguishably fast. Now, if we use the ^{13}C NMR of chemisorbed CO as the baseline for a comparison, then the spin–lattice relaxation rate, 19 s^{-1} , observed for the ^{77}Se of Au-surface-bound octaneselenol is even faster than that of chemisorbed ^{13}CO ($\sim 7 \text{ s}^{-1}$) on a Pt surface,¹⁶ even though the nuclear gyromagnetic ratio of the latter is 1.3 times larger than the former. This is also the case if the spin–spin relaxation rates are compared. Thus, we strongly believe that the remarkably efficient ^{77}Se nuclear spin relaxations observed here can be rationalized in the same fashion as for the ^{13}C NMR of the CO chemisorbed on transition metal surfaces. That is, the Se atom acquires a locally nonzero E_F -LDOS upon binding to the Au nanoparticle surfaces. Additional evidence supporting such a conclusion is presented in Figure 2C in which some typical ^{77}Se spin–lattice relaxation rates are plotted against the NMR shifts. It clearly shows that the spin–lattice relaxation rate increases as the NMR shift becomes more positive, which is a typical behavior when the variation in NMR shift is dominated by the conducting-electron-determined Knight shift.¹⁷ Such a behavior is again in great contrast to that of $^{13}\text{C}_1$ in octanethiol-protected Au nanoparticles where a more or less invariant value was observed across the $^{13}\text{C}_1$ NMR spectrum.¹⁵

The solid curve in Figure 2C is a fit to the simplest Korringa relationship¹⁸ which is the fingerprint of a metallic state:

$$T_1^{-1} = \left(\frac{T}{S}\right)(K - \delta_{\text{orb}})^2 \quad (1)$$

where $T = 298 \text{ K}$ is the absolute temperature at which T_1^{-1} is measured, $S = 7.16 \times 10^{-6} \text{ s} \cdot \text{K}$ is the Korringa constant for ^{77}Se , K is the total NMR shift, and δ_{orb} is the orbital (chemical) shift of the ^{77}Se used as the reference for the Knight shift. δ_{orb} is also the only fittable parameter. A value of $\delta_{\text{orb}} = -516 \pm 14 \text{ ppm}$ is obtained from the fit, which is quite reasonable, considering that it is entirely possible for the Se to acquire an anionic core structure upon surface bonding.¹⁹ While the simple model, eq 1, fails to account for the details, it does explain qualitatively the trend that

indicates the existence of a conducting-electron-caused Knight shift. The discrepancy suggests, however, that a theoretical framework more sophisticated than the simple, free electron model-based eq 1 is needed to interpret fully the ^{77}Se NMR data. Finally, it is worth noting that recent ab initio quantum calculations have indeed predicted a nonzero E_F -LDOS (0.64 states/eV) at the Se atom when bound to the Au surface.⁷ A definitive conclusion of a metallic state for Se–MAC can be obtained by temperature-dependent measurement of T_1 which is currently under way in our lab.

In summary, the results we have reported above are of general interest for at least two reasons. First, to the best of our knowledge, they represent the first observation of ^{77}Se NMR of octaneselenol-protected Au nanoparticles. This is of great importance for future molecular level studies of metal–MAC interactions by offering a powerful and the most proximal NMR probe to the metal–MAC interface. Second, at a more fundamental level, our NMR data strongly suggest that Se acquires nonzero E_F -LDOS upon binding to the Au nanoparticle surfaces, qualitatively consistent with the prediction of the recent ab initio quantum calculations.⁷ It is now feasible, in principle, to measure the E_F -LDOS at the metal–MAC interfaces using NMR techniques. It is expected, therefore, that the more detailed electronic-level information will soon be harnessed and these benchmark data will have profound chemical and physical ramifications in nanoscience in general and molecular electronics in particular.

Acknowledgment. Professor G. Chapman is gratefully acknowledged for his kind assistance in the TEM measurements. Financial support from Georgetown Graduate School Pilot Research Project Grant, Summer Grant, and Georgetown Startup as well as the PRF funds are gratefully acknowledged. B.S.Z. is a recipient of the 2003 NSF East Asia Summer Institute grant. T.Y. thanks JSPS for financial support.

References

- (1) Patrone, L.; Palacin, S.; Bourgoin, J. P.; J. Lagoute, T. Z. *Am. J. Chem. Phys.* **2002**, *281*, 325–332.
- (2) Samant, M. G.; Brown, C. A.; Gordon, J. G., II. *Langmuir* **1992**, *8*, 1615–1618.
- (3) Huang, F. K.; Horton, R. C., Jr.; Myles, D. C.; Garrell, R. L. *Langmuir* **1998**, *14*, 4802–4808.
- (4) Brust, M.; Stühr-Hansen, N.; Nørsgaard, K.; Christensen, J. B.; Nielsen, L. K.; Bjørnholm, T. *Nano Lett.* **2001**, *1*, 189–191.
- (5) Yee, C. K.; Ulman, A.; Ruiz, J. D.; Parikh, A.; White, H.; Rafailovich, M. *Langmuir* **2003**, *19*, 9450–9458.
- (6) Yaliraki, S. N.; Kemp, M.; Ratner, M. A. *J. Am. Chem. Soc.* **1999**, *121*, 3428–3434.
- (7) Di Ventura, M.; Lang, N. D. *Phys. Rev. B* **2002**, *65*, Art. No. 045402.
- (8) Seminario, J. M.; Zacarias, A. G.; Tour, J. M. *J. Am. Chem. Soc.* **1999**, *121*, 411–416.
- (9) Tour, J. M. *Acc. Chem. Res.* **2000**, *33*, 791–804.
- (10) Slichter, C. P. *Annu. Rev. Phys. Chem.* **1986**, *37*, 25–51.
- (11) Brust, M.; Walker, M.; Bethell, D.; Schiffrin, D. J.; Whyman, R. *J. Chem. Soc., Chem. Commun.* **1994**, 801–802.
- (12) Ruan, M. D.; Zhao, H. R.; Fan, W. Q.; Zhou, X. J. *J. Organomet. Chem.* **1995**, *485*, 19–24.
- (13) Zhao, X. R.; Ruan, M. D.; Fan, W. Q.; Zhou, X. J. *Synth. Commun.* **1994**, *24*, 1761–1765.
- (14) Hostetler, M. J.; Stokes, J. J.; Murray, R. W. *Langmuir* **1996**, *12*, 3604–3612.
- (15) Zelakiewicz, B. S.; de Dios, A. C.; Tong, Y. Y. *J. Am. Chem. Soc.* **2003**, *125*, 18–19.
- (16) Tong, Y. Y.; Rice, C.; Wieckowski, A.; Oldfield, E. J. *Am. Chem. Soc.* **2000**, *122*, 1123–1129.
- (17) Knight, W. D. In *Solid State Physics*; Turnbull, D., Ed.; Academic Press: New York, 1956; Vol. 2, pp 93–136.
- (18) Korringa, J. *Physica* **1950**, *XVI*, 601–610.
- (19) Mason, J., Ed. *Multinuclear NMR*; Plenum Press: New York, 1987.

JA049532W